



## Extreme ultraviolet photoionization of aldoses and ketoses

Joong-Won Shin<sup>a,c</sup>, Feng Dong<sup>a,c</sup>, Michael E. Grisham<sup>b,c</sup>, Jorge J. Rocca<sup>b,c</sup>, Elliot R. Bernstein<sup>a,c,\*</sup>

<sup>a</sup> Department of Chemistry, Colorado State University, Fort Collins, CO 80523-1872, USA

<sup>b</sup> Department of Electrical and Computer Engineering, Colorado State University, Fort Collins, CO 80523-1373, USA

<sup>c</sup> NSF Engineering Research Center for Extreme Ultraviolet Science and Technology, Colorado State University, CO 80523-1320, USA

### ARTICLE INFO

#### Article history:

Received 24 January 2011

In final form 9 March 2011

Available online 29 March 2011

### ABSTRACT

Gas phase monosaccharides (2-deoxyribose, ribose, arabinose, xylose, lyxose, glucose, galactose, fructose, and tagatose), generated by laser desorption of solid sample pellets, are ionized with extreme ultraviolet photons (EUV, 46.9 nm, 26.44 eV). The resulting fragment ions are analyzed using a time of flight mass spectrometer. All aldoses yield identical fragment ions regardless of size, and ketoses, while also generating same ions as aldoses, yields additional features. Extensive fragmentation of the monosaccharides is the result the EUV photons ionizing various inner valence orbitals. The observed fragmentation patterns are not dependent upon hydrogen bonding structure or OH group orientation.

© 2011 Elsevier B.V. All rights reserved.

### 1. Introduction

Functions of biological molecules depend upon their different isomeric forms and surrounding environments: these conformational structures are primarily governed by intricate balances among various inter- and intra-molecular interactions. Generation of biological molecules in the gas phase provides a convenient way for studying their individual properties, since they are free of all complicating interactions except for the intrinsic ones that determine molecular conformational freedom. These interactions often play significant roles in their photodissociation pathways, as was previously observed [1–7]. Many organic and biological molecules exposed to vacuum ultraviolet (VUV) radiation undergo isomer dependent fragmentation: different isomers can have different fragmentation patterns. Studies of fragmentation photochemistry of biological molecules have thus far been mostly limited to small bio/organic molecules [1–7], and the present work extends these studies to another class of important building blocks of life, the saccharides (also known as carbohydrates or sugars). In general, there are two classes of monosaccharides, aldoses (aldehyde saccharides) and ketoses (ketone saccharides); monosaccharides in each class are essentially isomers of one another with different OH orientations (Figure 1). Different intramolecular H bonding schemes are possible for each isomer. In a solution, a monosaccharide molecule can be in three different conformations: linear, 5-membered cyclic (furanose), or 6-membered cyclic (pyranose); the cyclic structures can adopt a chair or boat conformation. Each

conformer can additionally be either an  $\alpha$  or  $\beta$  anomer, depending upon the orientation of the OH at C1 (for aldose) or C2 (for ketose) anomeric centers. All these forms can coexist in a solution, but such structural complication is greatly simplified in the gas phase, for which the pyranose form is the dominant species, as demonstrated [8] through a reaction study of stereo selective ions and carbohydrate molecules. In addition, double resonance spectroscopy of phenyl attached carbohydrates [9–14] identified isomeric variations arising from different intramolecular H...O—H bonding schemes.

In the present study, we carry out photoionization mass spectrometry of three types of gas phase monosaccharides: 2-deoxyribose ( $C_5H_{10}O_4$ ) and aldopentoses [ $C_5(H_2O)_5$ , ribose, arabinose, xylose, lyxose]; aldohexoses [ $C_6(H_2O)_6$ , glucose, galactose]; and ketohexoses [ $C_6(H_2O)_6$ , fructose, tagatose]. Single photon ionization was achieved using 26.44 eV photons from a compact tabletop capillary discharge extreme ultraviolet (EUV) laser [15]. In light of the fact that fragmentation pathways of various biologically relevant molecules are conformer dependent [1–7], the purpose of the present study is to observe such behavior for the saccharides, which are in effect conformers of one another. To the best of our knowledge, this is the first experimental approach through which untagged, isolated saccharide molecules with the molecular formula of  $C_n(H_2O)_n$  are generated in the gas phase without the introduction of a solvent. The observed saccharide fragmentation patterns should thus be indicative of isolated, unsolvated molecules in their various conformational structures. Ionization processes and fragmentation pathways are explored by comparing the saccharide ionization behavior to that of tetrahydropyran. Various computational approaches are employed to explore the observed fragmentation patterns.

\* Corresponding author at: Department of Chemistry, Colorado State University, Fort Collins, CO 80523-1872, USA. Fax: +1 970 491 1801.

E-mail address: [erb@lamar.colostate.edu](mailto:erb@lamar.colostate.edu) (E.R. Bernstein).

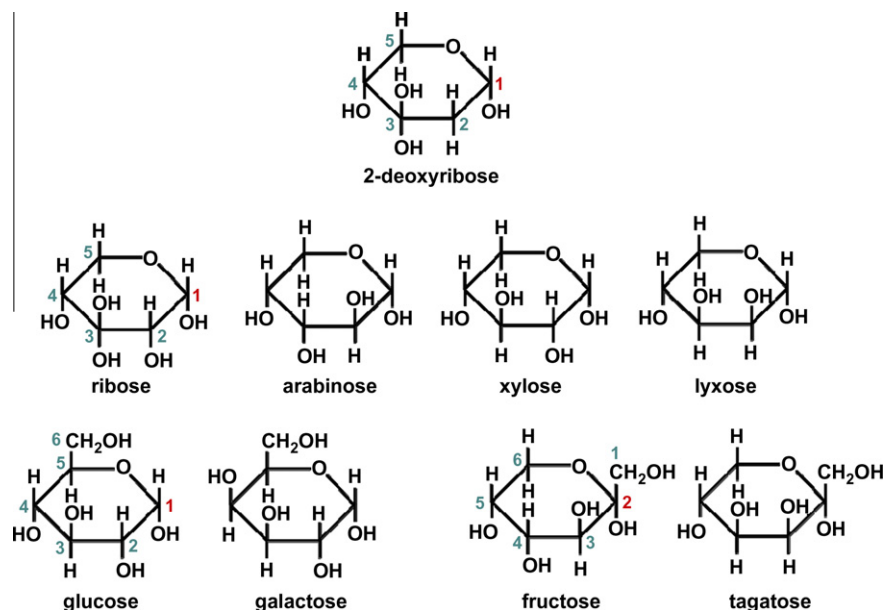


**Figure 1.** Haworth projections of monosaccharides with the  $\alpha$ -D-pyranose configuration. Ribose, arabinose, xylose, and lyxose are aldopentoses [ $C_5(H_2O)_5$ ], glucose and galactose are aldohexoses [ $C_6(H_2O)_6$ ], and fructose and tagatose are ketohexoses [ $C_6(H_2O)_6$ ]. The numbers in red indicate anomeric centers.

## 2. Experimental procedures

The monosaccharides used in the present study have the D configuration, and are not chemically tagged or labeled. Each saccharide powder is pressed into a pellet with a rhodamine 6G (R6G) matrix in a mixture of  $\sim$ 5:1 ratio (saccharide:R6G), and is softly desorbed with a 532 nm laser as it is rotated and translated by a motor to expose clean surface following each desorption pulse. The R6G molecules absorb the 532 nm photon energy and transfer heat to sample molecules during relaxation to vaporize them. We previously showed [16] that the desorption method does not fragment molecules, and fragment ions observed in the mass spectra are products of photoionization. The vaporized sample is supersonically expanded using pure He gas from a pulse nozzle and is collimated by a skimmer prior to entering the ionization region of a time of flight mass spectrometer. Tetrahydropyran is supersonically expanded by placing a reservoir filled with the 300 K liquid behind the pulse nozzle. Ionization energies (IE) of the monosaccharides are not known except for 2-deoxyribose, which has an IE of 10.51 eV [17]. This value is higher than our VUV radiation (118.2 nm, 10.49 eV) [18], and thus an EUV radiation (46.9 nm, 26.44 eV) [15,19] is employed for ionization of the saccharides. Tetrahydropyran has an IE of 9.46 eV [20], and thus can be ionized by both the VUV and EUV photons. The laser energy in the ionization region is less than  $\sim$ 1  $\mu$ J/pulse. Detailed descriptions for generation of VUV and EUV radiation are provided in Refs. [18,15,19], respectively.

## 3. Computational methods

Geometry optimization for a 2-deoxyribose molecule is carried out at the CAS(14,11)/6-31G level, and that for the cation is carried out at the CAS(13,11)/6-31G level. CAS calculations are suitable for accurate descriptions of molecular orbitals [7]. Based upon previous studies [8,21], only the chair conformation pyranose structure is considered. The numbers of electrons and orbitals in the active space are chosen to include all lone pair electrons on O atoms and electrons on the endocyclic C–C and C–O bonds. Koopmans' theorem ionization energy calculations for outer and inner valence

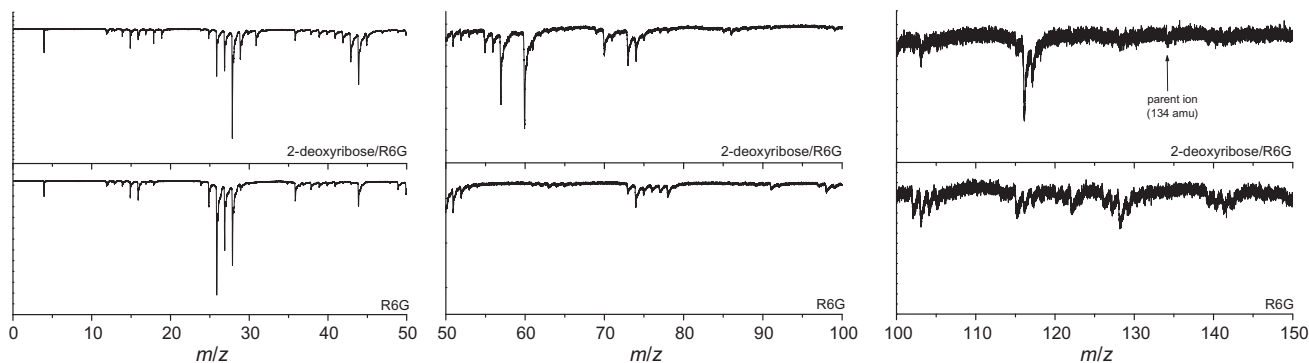
orbitals of 2-deoxyribose and tetrahydropyran are carried out by first optimizing their structures at the B3LYP/aug-cc-pVDZ level, and then performing electron propagator theory (outer valence Green's function propagator theory) calculations at the EPT/aug-cc-pVDZ level.

The calculations are carried out using the Gaussian 09 [22] program on the TeraGrid [23] supercomputer system.

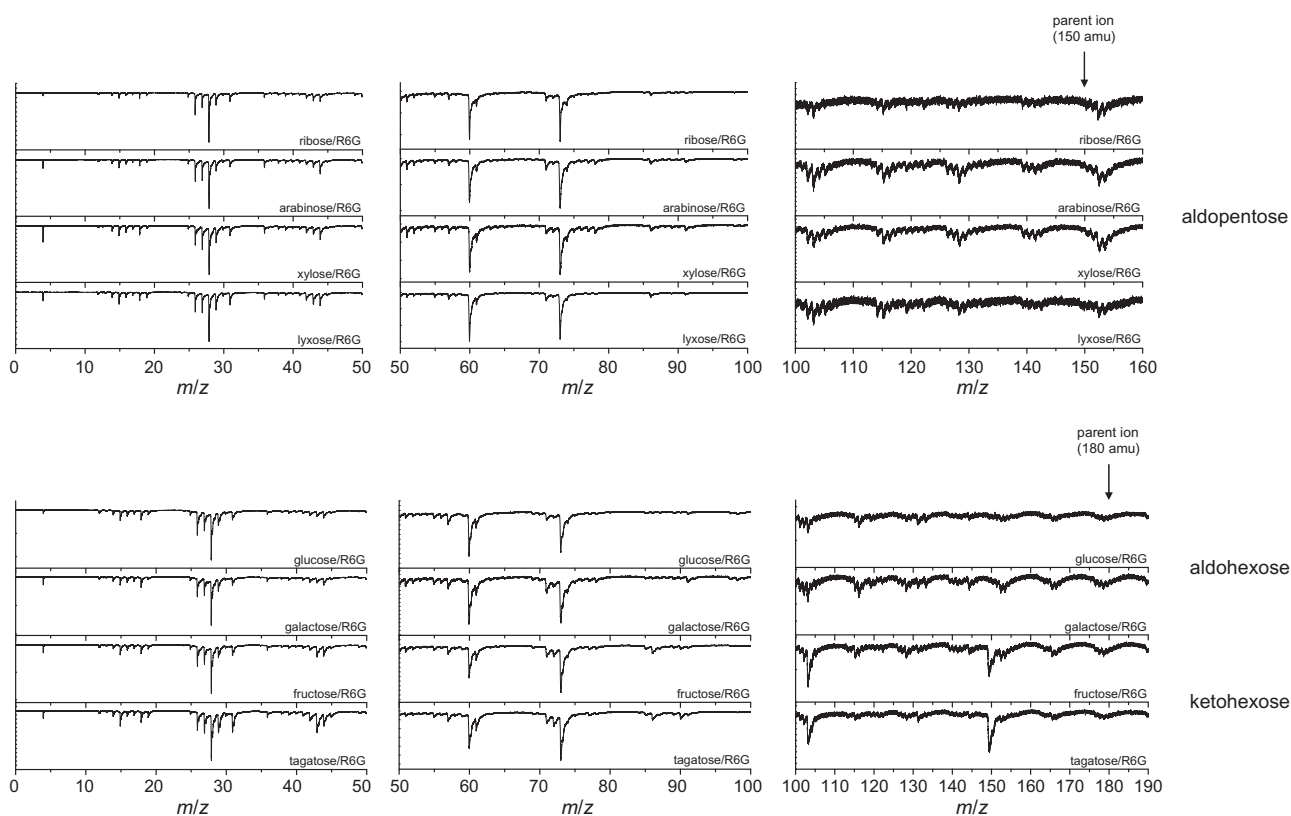
## 4. Results and discussion

Figure 2 shows the EUV photoionization mass spectrum of 2-deoxyribose, along with that of pure R6G to distinguish contributions from the matrix and background. Assignments of fragment ions of 2-deoxyribose (134 amu), based upon previous studies [16,20], are  $m/z = 18$  ( $H_2O^+$ ), 19 ( $H_3O^+$ ), 28 ( $C_2H_4^+$  or  $CO^+$ ), 29 ( $CHO^+$ ), 31 ( $CH_3O^+$ ), 42 ( $C_2H_2O^+$ ), 43 ( $C_2H_3O^+$ ), 55 ( $C_3H_3O^+$ ), 56 ( $C_3H_4O^+$ ), 57 ( $C_3H_5O^+$ ), 60 ( $C_2H_4O_2^+$ ), 70 ( $C_3H_2O_2^+$ ), 73 ( $C_3H_5O_2^+$ ), 86 ( $C_4H_6O_2^+$ ), 116 ( $C_5H_8O_3^+$ ), and 117 ( $C_5H_9O_3^+$ ). Distribution of fragmentations in our mass spectra is similar to and consistent with the previous studies [17,21,24–27] of 2-deoxyribose prepared and ionized under different conditions. Proposed fragmentation pathways imply highly complicated mass to charge ratio degeneracies that can arise from fragmentations at multiple sites in the molecule, and such extensive fragmentation indicates that chemical bonds in the 2-deoxyribose cation are prone to dissociation, with little dependence on isomeric structural variations. Indeed, a recent isotope substitution study [25] shows that all chemical bonds, both endocyclic and exocyclic, in the 2-deoxyribose molecule are susceptible to dissociation with slight but nonexclusive preference for the C5–O bond, and this suggests that each observed fragment ion in the current study arises from the parent ion fragmenting through multiple pathways.

Figure 3 presents the EUV photoionization mass spectrum of aldopentoses, aldohexoses, and ketohexoses. All aldopentoses yield identical fragment ions regardless of their structural differences (different OH group orientations and H bonding schemes), and the fragment ions are also nearly identical to those observed for 2-deoxyribose, except that loss of OH and  $H_2O$  from the parent ion is not observed for the aldopentoses. The reversed peak



**Figure 2.** EUV photoionization mass spectra of (upper panel) 2-deoxyribose/R6G and (lower panel) pure R6G. R6G is the matrix for enhancing laser desorption efficiency of the monosaccharide sample. The 2-deoxyribose parent ion is not observed.



**Figure 3.** EUV photoionization mass spectra of aldopentoses, aldohexoses, and ketohexoses mixed with R6G. R6G is the matrix for enhancing laser desorption efficiency of the monosaccharide samples. No fragment ion peaks associated with aldoses are observed in the higher mass region ( $m/z > 100$ ), and the parent ion is not observed for any of the monosaccharides.

intensities for  $C_3H_5O^+$  ( $m/z = 57$ ) and  $C_3H_5O_2^+$  ( $m/z = 73$ ) observed for 2-deoxyribose and aldopentoses result from their mass difference (134 and 150 amu). 2-deoxyribose and aldopentoses share similar extensive fragmentation pathways, and the presence of an OH at the C2 position of aldopentoses, and any possible H bonding interactions arising from its presence, does not play a notable role in their overall photochemistry. Interestingly, aldopentoses and aldohexoses generate the same fragment ions upon ionization, despite the presence of additional  $CH_2O$  (30 amu) at the C5 position of the aldohexoses. The fact that fragment ions observed for aldohexoses do not shift by  $m/z = 30$  means that dissociation of  $CH_2O$  from the parent ion occurs concurrently with all other fragmentation processes, thereby yielding the same fragment ions as aldopentoses. This further suggests that chemical bonds at the C5

position are particularly vulnerable to dissociation. As in the case of aldopentoses, no H bonding or OH orientation dependence is observed.

In the case of ketohexoses, while most fragment ions in the  $m/z = 10$ – $100$  range are identical to those of aldoses, several distinct features are observed. The ratio between  $C_2H_4O_2^+$  ( $m/z = 60$ ) and  $C_3H_5O_2^+$  ( $m/z = 73$ ) peak intensities is about 0.66 for ketohexoses, whereas the ratio is about one for all aldoses. This implies preferential (or suppressed) generation of the  $C_3H_5O_2^+$  (or  $C_2H_4O_2^+$ ) for ketohexoses. Also, additional fragments  $C_4H_7O_3^+$  and  $C_5H_9O_5^+$  are observed at  $m/z = 103$  and 149, respectively. The primary structural difference (Figure 1) between an aldose and a ketose is that OH and H are bonded to the anomeric C (C1) in an aldose, whereas OH and  $CH_2OH$  are bonded to the anomeric C (C2) in a ketose, and

this leads to the additional fragmentation pathways.  $C_5H_9O_5^+$  results from loss of  $CH_2OH$  from the C2 position, but loss of  $CH_2OH$  only is not observed for aldohexoses, in which the functional group is at the C5 position.  $C_4H_7O_3^+$  results from concurrent loss of  $C_2H_4O_2$  and OH, and this reaction is also not observed for aldoses. The type of functional groups present at the anomeric center affects monosaccharide fragmentation pathways, while H bonding interactions do not play any significant role, as inferred from the fact that all the monosaccharides within a class generate the same fragment ions following ionization. The above described behavior of saccharide ions can be seen in stark contrast to the behavior of amino acids [4] and  $\alpha$ -substituted carboxylic acids [7], which evidence fragmentation patterns upon VUV ionization that are exquisitely sensitive to neutral ground state conformation and intramolecular H bonding.

The reason for extensive fragmentation of monosaccharides is that EUV photons ionize both the outermost valence orbital (highest occupied molecular orbital, HOMO) and inner valence orbitals (HOMO-1, HOMO-2, etc.), each of which can lead to different dissociation pathways following ionization [28–34]. Comparison of VUV and EUV ionization mass spectra for tetrahydropyran reveals such an effect, as presented in Figure 4. When tetrahydropyran ( $C_5H_{10}O$ ), which is an analogue of the 6-membered cyclic monosaccharide, is ionized with VUV radiation, only the parent ion ( $m/z = 86$ ) is predominantly observed with very weak fragment ion intensities, but ionization with EUV radiation leads to extensive fragmentation with only a small amount of the parent ion remaining intact. Thus, increasing the photon energy leads to highly complicated fragmentation, which leads to the generation of  $m/z = 27$  ( $C_2H_3^+$ ), 28 ( $C_2H_4^+$ ), 29 ( $C_2H_5^+$ ), 39 ( $C_3H_3^+$ ), 41 ( $C_3H_5^+$ ), 45 ( $C_2H_5O^+$ ), 55 ( $C_3H_3O^+$ ), 56 ( $C_3H_4O^+$ ), and 85 ( $C_5H_9O^+$ ) fragment ions. Similar behavior is observed for many bio/organic molecules [28–39] as well as for 2-deoxyribose [21], all of which display additional fragment ions as ionizing photon energies increase. Both VUV and EUV photon energies are greater than the IE of tetrahydropyran and the laser energy is less than  $\sim 1 \mu\text{J}/\text{pulse}$  in the ionization region, so the ionization is a single photon process with the excess energy removed as the photoelectron kinetic energy ( $E_{KE} = E_{h\nu} - E_{BE}$ ). Therefore, the tetrahydropyran fragment ions are generated as singly charged incipient ions created as the vertical ion evolves from the Franck–Condon to adiabatic geometry, and not a result of multiphoton ionization/dissociation.

This observation implies that the EUV photons employed in the current study are ionizing inner valence orbitals of the monosaccharides (as well as the outermost valence orbital): this supposition is supported by Koopmans' theorem computational results from B3LYP/aug-cc-pVDZ//EPT/aug-cc-pVDZ calculations. As presented in Table 1, both the tetrahydropyran and 2-deoxyribose

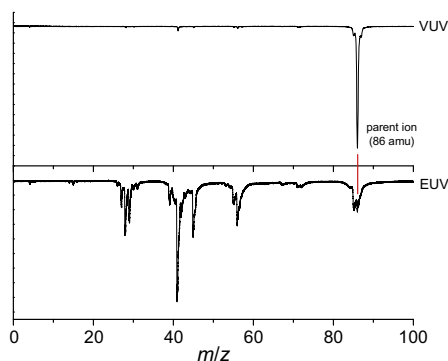


**Figure 4.** (Upper panel) VUV and (lower panel) EUV photoionization mass spectra of tetrahydropyran.

**Table 1**

Ionization energies of chair conformers of tetrahydropyran and 2-deoxyribose calculated at the B3LYP/aug-cc-pVDZ//EPT/aug-cc-pVDZ level of theory. Reported values are Koopmans' theorem results obtained from the electron propagator theory (outer valence Green's function propagator theory) calculations. Note that this method calculates ionization energies up to 20 eV.

Orbital	Ionization energy (eV)	
	Tetrahydropyran	2-Deoxyribose
HOMO	10.935	11.201
HOMO-1	12.070	12.089
HOMO-2	12.401	12.739
.	13.037	13.036
.	13.465	13.670
.	14.561	13.855
.	14.659	14.168
.	15.492	14.985
.	16.533	15.304
.	16.963	15.557
.	17.212	16.485
.	18.262	16.689
.	20.859	17.377
		17.527
		17.860
		18.645
		19.708
		20.249

molecules have many valence orbitals with IEs below 20 eV, all of which can be ionized with 26.44 eV photons. Similar observations have been made by soft X-ray photoelectron spectroscopy of a number of biomolecules [29,33,40,41]. Monosaccharide cation forms are not stable because their parent ions are not observed regardless of valence states. Thus, EUV ionization of saccharides occurs at least partially at the endocyclic C=C and C=O bonds, as ionization of a nonbonding orbital, such as those on the OH groups, does not readily lead to dissociation [33].

Such a mechanism is further suggested by a CAS(14,11)/6-31G calculation, which shows for 2-deoxyribose that the HOMO and inner valence orbitals are mostly centered on the endocyclic C–C and C–O bonds, as shown in Figure 5, from which photoelectrons are ejected upon EUV ionization. In the case of the HOMO, the electron density is located primarily on the C4–C5 bond. CAS(13,11)/6-31G optimization of the adiabatic ion with one electron in the HOMO (singly occupied molecular orbital, SOMO) shows that bond breaking indeed occurs at the C4–C5 bond (Figure 5 inset). While exploring inner valence states in a similar manner is not feasible with our currently available computational resources, the calculations involving the HOMO infer that endocyclic bond dissociation also occurs when inner orbitals are ionized, and that the ring opening is the initial step toward the highly complicated fragmentation pathways. Absence of the parent ion most likely arises from the presence of one or more repulsive unbound potential energy surfaces, which leads to complete electronic predissociation of the parent ion. The presence of repulsive states that cross parent ion potential energy surfaces is necessary considering our B3LYP/aug-cc-pVDZ calculations that the energy difference between the Franck–Condon and adiabatic states is only 0.48 eV (at the HOMO level). This difference is insufficient to overcome the C–C bond strength of 3.61 eV [42] during ion relaxation to the vibrational ground state, and the most likely pathway is through crossing of repulsive states below the dissociation limit of the parent ion potential energy surface.

Extensive fragmentation can also result from Coulomb explosion of multiply charged ions, which are generated following Auger cascades after inner orbitals of molecules are ionized by high energy photons in the EUV or X-ray regions. Such a scenario is possible, however, only with photon energies greater than 40 eV [43], and requires ionization of deep inner orbitals, such as those at core levels [44–48]. Thus, the saccharide fragment ions observed in the current study are very unlikely the result

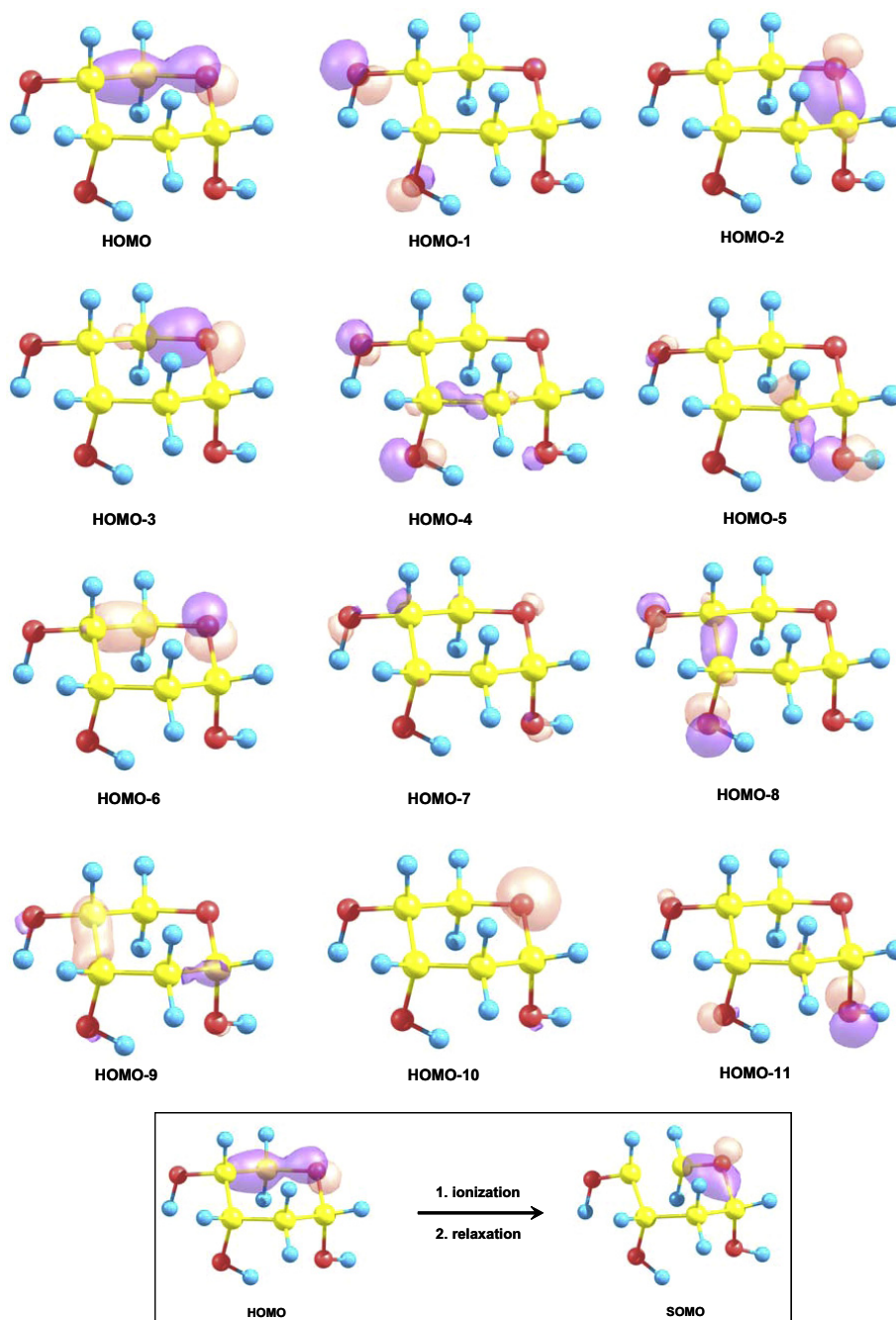


**Figure 5.** CAS(14,11)/6-31G structures and molecular orbitals of 2-deoxyribose, and CAS (13,11)/6-31G structure and molecular orbital of 2-deoxyribose parent ion. Structures in the inset at the bottom compare the neutral ground state and adiabatic ion state involving the HOMO. HOMO = highest occupied molecular orbital; SOMO = singly occupied molecular orbital.

of Coulomb explosion, as supported by consideration of energy conservation. According to our B3LYP/aug-cc-pVDZ calculations, the energy difference between singly and doubly charged Franck–Condon 2-deoxyribose ions is 15.36 eV. This is the minimum energy required to remove an electron from a singly charged ion. Assuming that the EUV laser ionizes an inner valence orbital with 26.44 eV IE and that an electron from the HOMO decays into the ionized orbital, an excess energy of 15.93 eV (26.44 – 10.51 eV; 10.51 eV is the experimentally obtained IE [17]) is generated. This is the maximum energy that can be generated from an Auger transition. The calculations show that although the minimum energy for the second ionization is less than the maximum energy that can be attained from the Auger

decay (15.36 vs. 15.93 eV), the two values are very close, and the maximum energy decreases when the decay occurs from a HOMO-*n* orbital. Therefore, even if decays occur, those involving deep inner valence orbitals cannot generate multiply charged parent ions, and while those involving outer valence orbitals may generate multiply charged ions, the contribution to the overall fragmentation behavior of the saccharides would be insignificant.

## 5. Conclusions

We have successfully generated isolated, untagged monosaccharide molecules in the gas phase without using a solvent. The

mass spectral data and computational results show that 26.44 eV EUV photons access several valence states of the monosaccharide molecules, leading to generation of many fragment ions. All aldoses (aldopentoses and aldohexoses) yield the same ions through similar fragmentation processes, whereas aldoses and ketoses yield similar but slightly different mass spectra due to the presence of different functional groups at their anomeric centers. Differences in conformational freedom such as the H bonding interaction and OH group orientation play little, if any, role in fragmentation behavior following ionization, and generation of the same fragment ions with nearly identical mass spectral intensities within each type (aldose and ketose) suggests that ion fragmentation pathways are the same for each. Furthermore, the similarity between the mass spectrum of 2-deoxyribose and those of other monosaccharides indicates that bond dissociation in the latter molecules is also not site specific, but occurs at all chemical bonds.

Application of an EUV laser to saccharide photochemistry in the gas phase is a promising fundamental approach for investigating how biological molecules respond to high energy radiation. A greater variety of biomolecules is currently being investigated using similar approaches described in this work, and a series of infrared (IR) experiments are being set up to find possible threshold and structural fragmentation pathways.

#### Acknowledgments

This study is generously supported by ARO (W911NF-10-1-0117) and NSF Center for Extreme Ultraviolet Science and Technology (EEC-0310717).

#### References

- [1] S.T. Park, S.K. Kim, M.S. Kim, *Nature* 415 (2002) 306.
- [2] K.-W. Choi, D.-S. Ahn, J.-H. Lee, S.K. Kim, *Chem. Commun.* (2007) 1041.
- [3] M.H. Kim, L. Shen, H. Tao, T.J. Martinez, A.G. Suits, *Science* 315 (2007) 1561.
- [4] Y. Hu, E.R. Bernstein, *J. Chem. Phys.* 128 (2008) 164311.
- [5] S. Choi, T.Y. Kang, K.-W. Choi, S. Han, D.-S. Ahn, S.J. Baek, S.K. Kim, *J. Phys. Chem. A* 112 (2008) 5060.
- [6] L. Zhang et al., *J. Phys. Chem. A* 113 (2009) 5838.
- [7] A. Bhattacharya, J.-W. Shin, K.J. Clawson, E.R. Bernstein, *Phys. Chem. Chem. Phys.* 12 (2010) 9700.
- [8] L.P. Guler, Y.-Q. Yu, H.I. Kenttämaa, *J. Phys. Chem. A* 106 (2002) 6754.
- [9] F.O. Talbot, J.P. Simons, *Phys. Chem. Chem. Phys.* 4 (2002) 3562.
- [10] P. Çarçalbal et al., *J. Am. Chem. Soc.* 127 (2005) 11414.
- [11] I. Hünig et al., *Phys. Chem. Chem. Phys.* 7 (2005) 2474.
- [12] J.P. Simons, R.A. Jockusch, P. Çarçalbal, I. Hünig, R.T. Kroemer, N.A. Macleod, L.C. Snoek, *Int. Rev. Phys. Chem.* 24 (2005) 489.
- [13] P. Çarçalbal et al., *Phys. Chem. Chem. Phys.* 8 (2006) 129.
- [14] J.P. Simons, *Mol. Phys.* 107 (2009) 2435.
- [15] S. Heinbuch, M. Grisham, D. Martz, J.J. Rocca, *Opt. Express* 13 (2005) 4050.
- [16] J.-W. Shin, E.R. Bernstein, *Trends Appl. Spectrosc.* 7 (2009) 47.
- [17] S. Ptasińska, S. Denifl, P. Scheier, T.P. Märk, *J. Chem. Phys.* 120 (2004) 8505.
- [18] J.-W. Shin, E.R. Bernstein, *J. Chem. Phys.* 130 (2009) 214306.
- [19] F. Dong, S. Heinbuch, J.J. Rocca, E.R. Bernstein, *J. Chem. Phys.* 124 (2006) 224319.
- [20] A.A. Planckaert, J. Doucet, C. Sandorf, *J. Chem. Phys.* 60 (1974) 4846.
- [21] G. Vall-Ilosera, M.A. Huels, M. Coreno, A. Kivimäki, K. Jakubowska, M. Stankiewicz, E. Rachlew, *ChemPhysChem* 9 (2008) 1020.
- [22] M.J. Frisch et al., *Gaussian 09, Revision A.02*, Gaussian, Inc., Wallingford, CT, 2009.
- [23] C. Catlett et al., *TeraGrid: Analysis of Organization, System Architecture, and Middleware Enabling New Types of Applications*, in: L. Grandinetti (ed.), *HPC and Grids in Action, IOS Press Advances in Parallel Computing Series*, Amsterdam (2007).
- [24] Z. Deng, I. Bald, E. Illenberger, M.A. Huels, *Phys. Rev. Lett.* 95 (2005) 153201.
- [25] I. Bald, Z. Deng, E. Illenberger, M.A. Huels, *Phys. Chem. Chem. Phys.* 8 (2006) 1215.
- [26] F. Alvarado, S. Bari, R. Hoekstra, T. Schlathölder, *Phys. Chem. Chem. Phys.* 8 (2006) 1922.
- [27] Z. Deng, I. Bald, E. Illenberger, M.A. Huels, *J. Chem. Phys.* 127 (2007) 144715.
- [28] S. Pilling, A.F. Lago, L.H. Coutinho, R.B. de Castilho, G.G.B. de Souza, A. Naves de Brito, *Rapid Commun. Mass Spectrom.* 21 (2007) 3646.
- [29] O. Plekan, V. Feyer, R. Richter, M. Coreno, K.C. Prince, *Mol. Phys.* 106 (2008) 1143.
- [30] M. Geronés, M.F. Erben, R.M. Romano, C.O. Della Védova, L. Yao, M. Ge, *J. Phys. Chem. A* 112 (2008) 2228.
- [31] M. Geronés, A.J. Downs, M.F. Erben, M. Ge, R.M. Romano, L. Yao, C.O. Della Védova, *J. Phys. Chem. A* 112 (2008) 5947.
- [32] O. Plekan et al., *Phys. Scr.* 78 (2008) 058105.
- [33] V. Feyer, O. Plekan, R. Richter, M. Coreno, K.C. Prince, *Chem. Phys.* 358 (2009) 33.
- [34] K.B. Bravaya, O. Kostko, S. Dolgikh, A. Landau, M. Ahmed, A.I. Krylov, *J. Phys. Chem. A* 114 (2010) 12305.
- [35] L.H. Coutinho, M.G.P. Homem, R.L. Cavasso-Filho, R.R.T. Marinho, A.F. Lago, G.G.B. de Souza, A. Naves de Brito, *Braz. J. Phys.* 35 (2005) 940.
- [36] O. Plekan, V. Feyer, R. Richter, M. Coreno, M. de Somine, K.C. Prince, *Chem. Phys.* 334 (2007) 53.
- [37] Y. Pan, L. Zhang, T. Zhang, H. Guo, X. Hong, L. Sheng, F. Qi, *Phys. Chem. Chem. Phys.* 11 (2009) 1189.
- [38] H. Guo, L. Zhang, L. Deng, L. Jia, Y. Pan, F. Qi, *J. Phys. Chem. A* 114 (2010) 3411.
- [39] L. Deng, L. Zhang, H. Guo, L. Jia, Y. Pan, H. Yin, F. Qi, *J. Mass Spectrom.* 45 (2010) 734.
- [40] O. Plekan, V. Feyer, R. Richter, M. Coreno, M. de Simone, K.C. Prince, V. Carravetta, *J. Phys. Chem. A* 111 (2007) 10998.
- [41] V. Feyer, O. Plekan, R. Richter, M. Coreno, K.C. Prince, V. Carravetta, *J. Phys. Chem. A* 113 (2009) 10726.
- [42] D. Voet, J.G. Voet, C.W. Pratt, *Fundamentals of Biochemistry*, John Wiley & Sons, Inc., New York, NY, 1999, pp. 25.
- [43] K. Ueda, J.H.D. Eland, *J. Phys. B: At. Mol. Opt. Phys.* 38 (2005) S839.
- [44] R.R.T. Marinho, A.F. Lago, M.G.P. Homem, L.H. Coutinho, G.G.B. de Souza, A. Naves de Brito, *Chem. Phys.* 324 (2006) 420.
- [45] A. Sugishima et al., *J. Chem. Phys.* 131 (2009) 114309.
- [46] M. Alagia et al., *J. Phys. Chem. A* 113 (2009) 14755.
- [47] Z.D. Pešić, D. Rolles, I. Dumitriu, N. Berrah, *Phys. Rev. A* 82 (2010) 013401.
- [48] H. Iwayama, K. Nagaya, H. Murakami, Y. Ohmasa, M. Yao, *J. Phys. B: At. Mol. Opt. Phys.* 43 (2010) 185207.